SAND2008-7431C

Effect of Base Material and Plating Layers on the Mechanical Strength of Au-Sn Solder Bonds

P. Vianco, G. Zender, and A. Kilgo
Sandia National Laboratories[1], Albuquerque, NM USA
ptvianc@sandia.gov: 505-844-329

Abstract

A study was conducted to identify the root-cause of low pull strengths that were experienced by phosphor bronze (Cu-Sn-P) edge pins on a low-temperature co-fired (LTCC) ceramic substrate. The pins were attached to post-process, fired-on Au thick film bond pads, using the 80Au-20Sn (wt.%) solder. Root-cause failure analysis identified the formation of a high-Sn $(Au, Ni)_xSn_y$ reaction layer at the pin/solder interface. The reaction layer weakened the joint due to the low interfacial bond strength between it and the electroplated Ni layer. The presence of Cu in the Au layer from the Cu-Sn-P pin material either, alone or via a synergistic with low-level Ni contamination in the Au layer, drove the diffusion of an excess quantity of Sn from the solder to the pin/solder interface, thereby generating the $(Au, Ni)_xSn_y$ reaction layer. A successful mitigation process was to recondition the Cu-Sn-P pins by stripping away the original Au coating from the pin surfaces; then plating an additional 1.2 – 1.5 µm Ni layer over the previous Ni coating; and lastly plating a new Au layer (1.5 µm) over that new Ni finish. The Au-Sn solder joints that were made using these reconditioned pins, exhibited excellent pull strength performance for subsequent LTCC units.

Introduction

Gold-tin solder in electronic packaging (structural)
The 80Au-20Sn (wt.%) solder (abbreviated Au-Sn) has been used for a number of structural applications within the electronics packaging industry [1 – 3]. This particular alloy has the eutectic composition with equivalent solidus and liquidus temperatures (T_s and T_l, respectively) of 278°C [4]. The relatively high solidus temperature allows the Au-Sn alloy to be used in the assembly of high-temperature components or as the high-temperature attachment within a step-soldering operation. An example of the latter case in electronic packaging is the use of the Au-Sn alloy as a Si die attach material or as a lid seal filler metal. A lid sealing application is shown in Fig. 1.

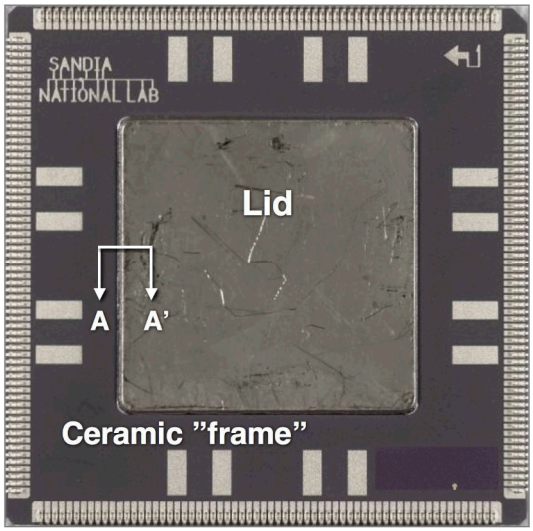

(a)

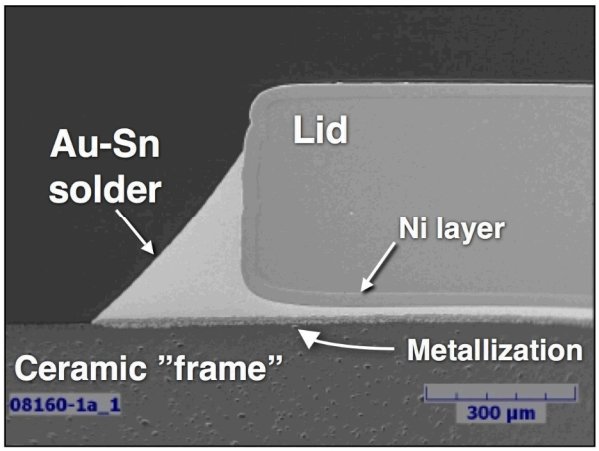

(b)

Fig. 1 (a) Stereo photograph of a ceramic package that uses a Au-Sn solder to attach the lid to the frame. (b) SEM photograph showing the Au-Sn solder joint between the lid and the ceramic frame indicated by section view A-A'.

The lid and ceramic "frame" are shown in Fig. 1a. The scanning electron microscope (SEM) photograph in Fig. 1b shows the fillet and completed gap (section A-A') that provide

[1] Sandia is a multiprogram laboratory operated by Sandia Corporation, a Lockheed Martin Company, for the United States Department of Energy's National Nuclear Security Administration under Contract No. DE-AC04-94AL85000.

the hermetic seal for the package (frame) interior. An electroplated Ni layer is often used on lids to provide a pristine solderable surface onto which, the molten Au-Sn solder wets. When used in a step-soldering application, the Au-Sn solder joint would not remelt during a second-level assembly that attaches the package in Fig. 1a to a circuit board using the eutectic 63Sn-37Pb (Sn-Pb) alloy ($T_s = T_l = 183°C$). Also, the Au-Sn solder exhibits excellent out-gassing properties for the interior volume of the package, making it well suited for optoelectronic as well as micro-electrical-mechanical systems (MEMS) assembly applications.

The Au-Sn solder has a very high strength, allowing it to provide a very robust, structural joint. Consequently, the ductility of this solder is very low. Yet, the Au-Sn solder exhibits excellent fatigue resistance properties [5]. A particular attribute of the Au-Sn solder is that, owing to its high Au content, the solder is slow to oxidize. Therefore, when processed in an inert atmosphere (e.g., N_2), the molten Au-Sn will readily wet to other Au-base materials or to Au-finishes, thereby eliminating the need for a flux. However, when exposed to air, a thin Sn oxide "skin" will develop on the molten Au-Sn surface that can impede the wetting process. Mechanical agitation or slight pressure will readily break the skin so as to allow the wetting process to take place. Also, the Au-Sn solder has a considerably higher surface tension than do other Sn-based solders [6]. As a result, it does not readily spread over the joint faying surfaces, particularly in the absence of a flux. Therefore, mechanical pressure is also required to force the solder to spread as well as to eliminate voids that can be difficult to extract from the gap. It is not uncommon to have a moderate number of voids in Au-Sn solder joints, particularly because these joints are made with preplaced, solder preforms or a solder paste. The use of preforms or paste offers very little flow behavior by the molten solder, resulting in the incorporation of air and/or volatiles trapped between the base material faying surfaces.

Multi-chip module edge pin attachment application

The application, which is the basis of the study presented here, utilized the Au-Sn solder to attach edge pins onto the Au thick film bond pads of a low-temperature co-fired ceramic (LTCC) multi-module unit. The assembly is shown in Fig. 2a. The edge pins are shown at the bottom of the unit. The Au-Sn solder is part of a step-soldering operation for this unit. In this case, the edge pin Au-Sn solder joints are required to not melt during two Sn-Pb soldering processes: (1) attachment of the Si dice to the LTCC substrate and (2) attachment of the module to a cable via the leads at the ends of the pins.

A high magnification, SEM photograph of an edge pin solder joint is shown in Fig. 2b. The pin is attached to the thick film bond pad using the Au-Sn solder. There is evidence of flow of the solder to the top of the pin, indicating excellent solderability of the latter's Au and Ni coatings. A metallographic cross section of the edge pin solder joint is shown in Fig. 3. The extent of voiding is large relative to that experienced when using solder preforms in other applications (Fig. 1b). Yet, owing to the strength of the solder, the Au-Sn joint as depicted provided adequate strength for the pin, despite the voids.

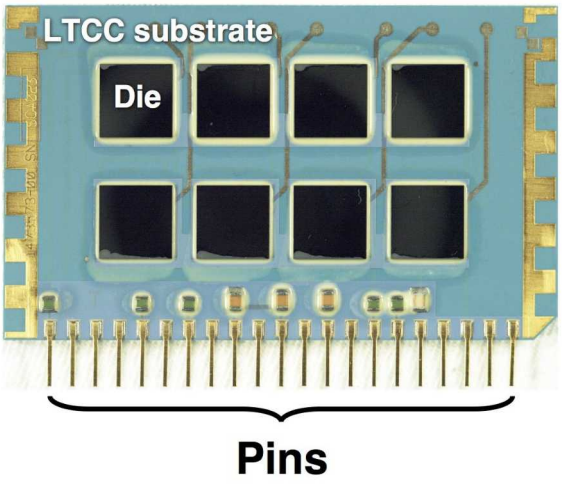

(a)

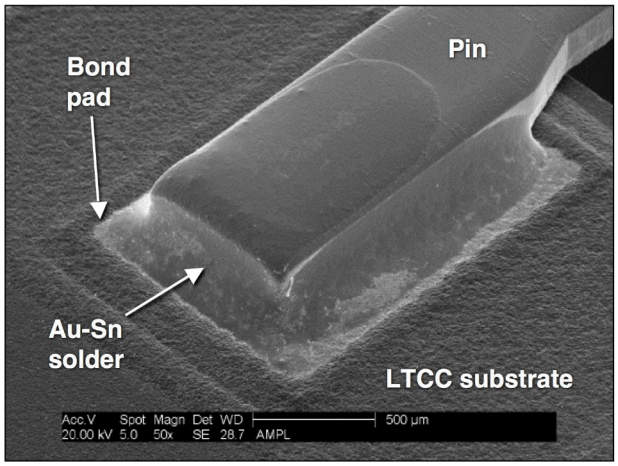

(b)

Fig. 2 (a) Stereo photograph of the module and the pins soldered to pads along the bottom edge. (b) SEM photograph of the edge pin soldered to the thick film bond pad on the LTCC substrate using Au-Sn solder.

A higher magnification view of the Au-Sn solder joint microstructure is shown in Fig. 4. The dotted line

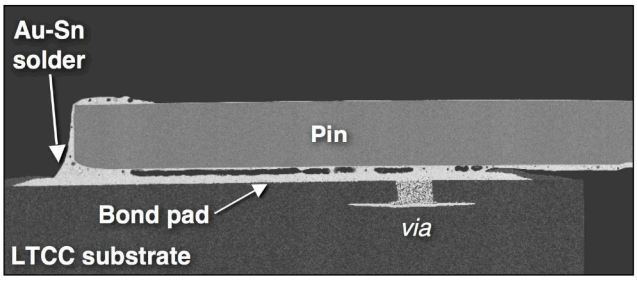

Fig. 3 SEM photograph showing the general structure of the pin, Au-Sn solder joint by means of a metallographic cross section.

distinguishes the thick film bond pad from the Au-Sn solder. The lead has a Ni solderable finish and Au protective finish. The latter was fully dissolved into the Au-Sn solder. The Au-Sn solder reacted with the electroplated Ni layer as part of the wetting process, establishing the bond to the lead. The reaction layer is visible at the pin/solder interface. This image exemplifies that excellent integrity of the interfaces.

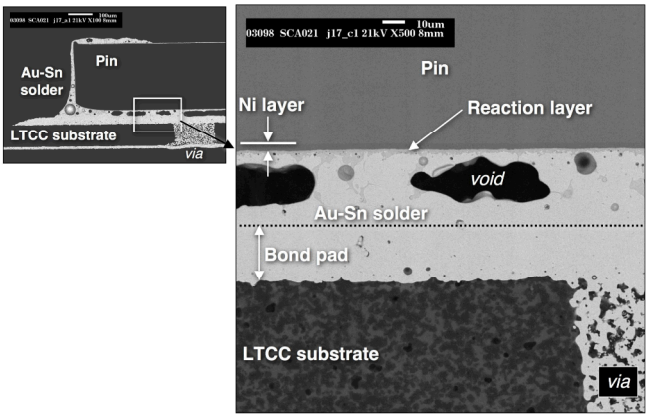

Fig. 4 SEM photograph of the microstructure of the Au-Sn solder bond attaching the pin to the LTCC bond pad. The dotted line delineates the Au-Sn solder from the Au thick film pad.

The pin solder joints were qualified by visual inspection and a pull test. The schematic diagram of the pull test configuration is shown in Fig. 5. Although the nomenclature "pull test" was used, in fact, the configuration was that of a *peel test*.

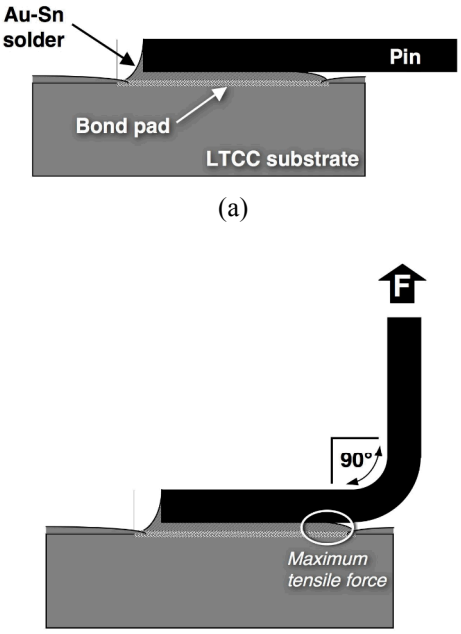

(a)

(b)

Fig. 5 Schematic diagram shows the pin pull test configuration: (a) the as-soldered pin and (b) bending of the pin lead and pull direction.

Nevertheless, the maximum pull load (force, F) is a suitable metric because it takes place when the applied load causes primarily a tensile force to the right-hand fillet of the joint (oval). The pull tests were performed on all twenty-one pins of an LTCC process monitor unit. The original acceptance criterion, which was in place when the case study was initiated, was a minimum pull strength of 1.5 lb per pin. Process and materials improvements raised the minimum strength metrics further in the program to: (a) an average pull test > 2.6 lb and (b) all individual pull tests having a strength > 2.2 lb.

An important task within the pull test procedure was analysis of the failure modes. The failure mode analysis determined the integrities of: (a) the Au-Sn solder within the gap (e.g., excessive void formation); (b) the several interfaces within the joint structure, and (c) the LTCC substrate. The two dominant failure modes are shown by the stereo and SEM photographs in Fig. 6.

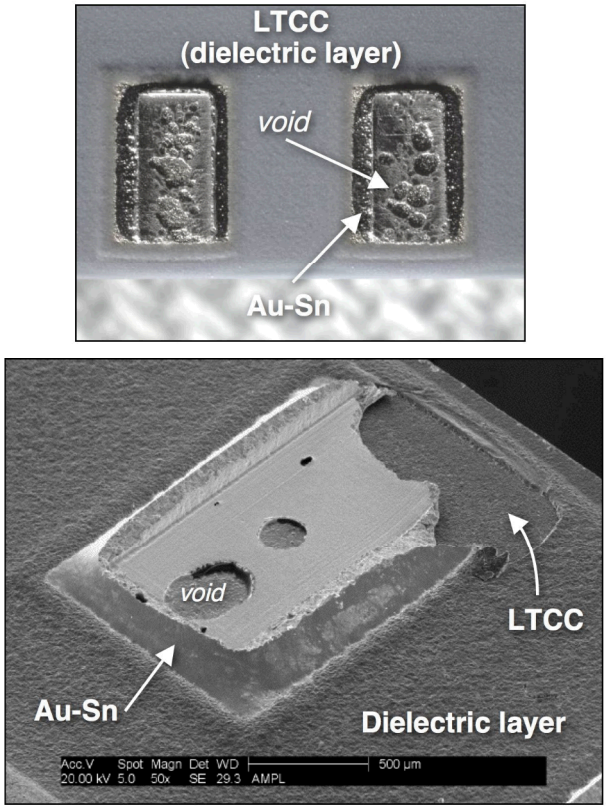

(a)

Fig. 6 Stereo and SEM photographs showing the two predominant failure modes of the pin, Au-Sn solder joint pull test: (a) pin/solder interface failure and (b) thick film/LTCC failure, including divots pulled from the LTCC substrate. *(con't)*

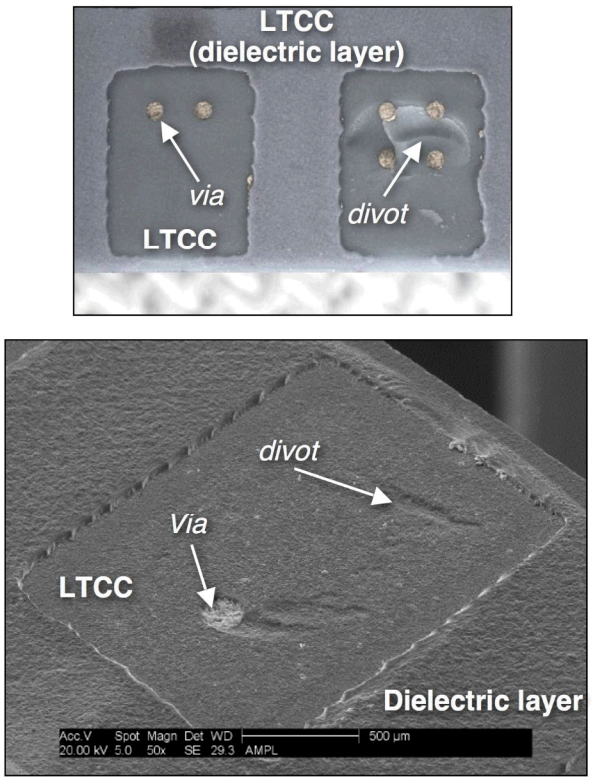

(b)

Fig. 6 Stereo and SEM photographs showing the two predominant failure modes of the pin, Au-Sn solder joint pull test: (a) pin/solder interface failure and (b) thick film/LTCC failure, including divots pulled from the LTCC substrate.

The less-frequently observed failure modes were fracture of the pin lead and failure within the Au-Sn solder, itself.

Problem

Materials system

The materials systems are described here. The pins were 0.254 mm thick phosphor bronze alloy (C510000: 94.8Cu-50Sn-0.2P, wt.%; ¾ hard). The specified electroplated Ni and Au finish thicknesses were 1.3 – 2.0 µm Ni and 2.0 – 5.0 µm Au.

The bond pad is 100%Au thick film layer. The layer is fired onto the LTCC in two post-process steps. The first step is the print-dry-fire of DuPont™ 5062 thick film, which is 100%Au plus the glass phase (trademark of E. I. DuPont de Nemours and Company Wilmington, DE). The 5062 thick film layer adheres to the LTCC surface by the glass phase that diffuses to the thick film/LTCC interface. The glass phase is generally so thin as to not be observable in SEM images. Then, a second print-dry-fire sequence is performed with the DuPont™ 5063 thick film ink. The metal composition is also 100%Au; but, it is of a greater concentration to improve solderability.

The solder is the 80Au-20Sn (wt.%) alloy. The pin is attached to a thick film bond pad using a Au-Sn solder *paste* that is placed between the pin and pad. (This process does not use a preform owing to the size constraint of the bond area.) The soldering process does not use a flux; it is performed in a belt furnace under a N_2 blanket.

The long, straight segment of the pin is subsequently soldered into a rigid-flex circuit board using a conventional 63Sn-37Pb solder processing.

Low pull strengths

During the course of the development of the pin connection to the LTCC substrate (bond pads), the Au-Sn solder joints experienced low pull strengths. The individual as well as mean pull strengths were less than 1 lb. The poor strengths were traced to several vendor lots. Stereo photographs of failure modes, which were similar to those in Fig. 6, when combined with the individual lead pull strength values, showed a correlation between low pull strength and a preference for the pin/solder failure mode that was shown in Fig. 6a. This correlation suggested that the root-cause of the low pull strengths rested with the interface between the solder and the pin rather than a failure of the Au-Sn solder (bulk) or at the thick film/LTCC interface.

Failure analysis methodology

An investigation was begun to determine the root-cause of the low pull strengths. The methodology included the following steps:

1. Perform SEM imaging and energy dispersive x-ray analysis (EDXA) of the fractures surfaces to determine the location of the fracture.
2. Conduct metallographic cross section evaluations of the pin solder joints, including those of pull-tested pins, to confirm the location of the fracture. The SEM was used to observe the solder microstructures due to some polishing relief generated by the different material hardness values across these joints.
3. Utilize electron probe microanalysis (EPMA) to map the elemental distributions within the joints. Such maps provide the means to identify phases within the joint that may impact the pull strength properties.

It was critical that the failure analysis not only identify the root-cause of the low pull strengths, but that it also be sufficiently in-depth so as to offer potential solutions to the problem under the constraints of the program requirements.

Fracture surface analysis

It was determined from the onset that the relatively high degree of porosity was not responsible for the low pull strengths. Thus, the analysis moved on to the fracture surfaces.

The SEM photograph in Fig. 7a shows the fracture surface of a pin that was pull tested from the substrate exhibiting a low strength. Energy dispersive x-ray analysis (EDXA) was used to determine, qualitatively, the composition of the various surface features. The voids are indicated by the original electroplated Au coating or by a thin layer of Au-Sn solder.

The predominant fracture surface exhibited elemental Ni that originated from the Ni solderable finish on the pin. The SEM image in Fig. 7b is that of the corresponding bond pad. The voids have the thin layer of Au-Sn solder that wetted the Au thick film bond pad. The predominant surface feature, which corresponded to the Ni surface on the pin, had the elements Au, Sn, and Ni.

The mode of separation, as determined from the morphology and chemistry of the fractures surfaces in Figs. 7a and 7b, is shown schematically in Fig. 7c. The predominant separation occurred between the electroplated Ni layer on the pin and a reaction layer comprised of Au, Ni, and Sn that formed between the Au-Sn solder and the Ni layer. And, in fact, this

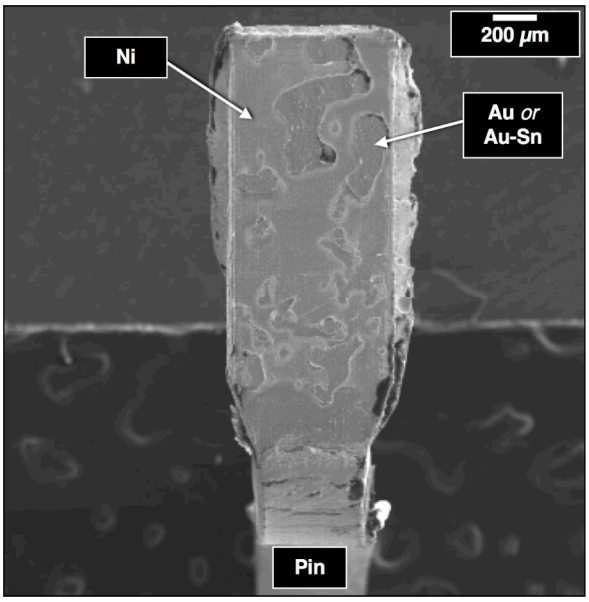

(a)

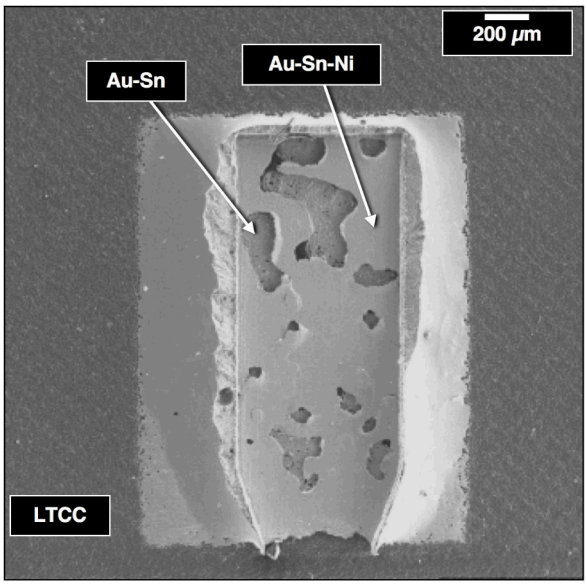

(b)

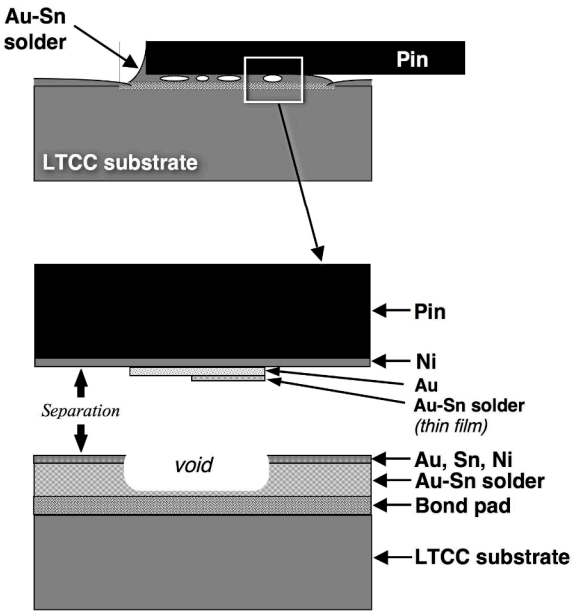

(c)

Fig. 7 SEM photographs of the fractures surfaces that are representative of pins exhibiting low pull strength: (a) the pin and (b) the pad. (c) Schematic diagram showing the separation and materials compositions as deciphered from the fracture surface morphologies and EDXA data.

failure mode was confirmed by metallographic cross section. Shown in Fig. 8 is an SEM photograph that captures the crack propagation path. It is clear that that path is between the remaining Ni coating on the pin and the reaction layer.

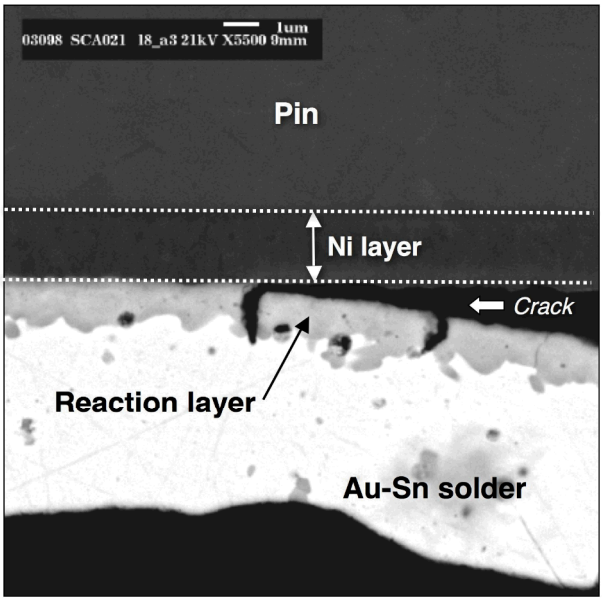

Fig. 8 SEM photograph that captures the crack path present during the low pull strength failure of the pin Au-Sn solder joint. The crack path is at the interface between the Ni coating on the pin and the reaction layer.

To this point, it appeared that the root-cause of the low pull strengths was associated with the solder/pin interface. Specifically, the weak structure was the interface between the electroplated Ni layer of the pin and a reaction layer that formed between the latter and the Au-Sn solder.

However, there remained a need to further analyze this problem for the following reason. The materials system comprised of Au-Sn solder wetted to an electroplated Ni (and Au protective finish) is very common in the electronics industry. Its successful history suggested that the present failure problem had extenuating circumstances. Additional details would also be required to determine a mitigation strategy for this solder joint. Therefore, a second phase of analyses was performed on the pin solder joints.

Second Phase Analysis

The first step was to determine a possible role of the Cu-Sn-P pin material on the joint mechanical properties. Towards this goal, similar LTCC units were fabricated with Au-Sn pin solder joints by a separate vendor. Those joints differed in the following manner:

1. The pin material was an Fe-Ni-Co alloy as opposed to Cu-Sn-P.
2. The Ni layer was replaced with a Co-Ni alloy.
3. The Au layer was 4.0 µm thick rather than approximately 1.5 – 2.0 µm.

Two groups were fabricated by the vendor. The solder joints of both groups exhibited excellent pull strengths, generally in the range of 1.6 – 2.0 lbs.

Shown in Fig. 9 are two stereo photographs (a, b) showing the two failure modes that were observed in the pull test. The predominant mode was that of "Joint 2". The "Joint 1" was cross-sectioned along the red line, which intercepted both the thick film/LTCC interface failure and, more importantly, the pin/solder interface. At the pin/solder interface, the fracture path was through the reaction layer between the Ni layer and the Au-Sn solder as shown by the SEM photograph (c). Therefore, it was concluded that (a) the presence of the reaction layer and (b) even when fracture occurred through the reaction layer, did not predispose the Au-Sn solder joint to a low pull strength.

These second-vendor experiments also offered the opportunity to address an alternative scenario. Owing to the thicker Au coating on the Fe-Ni-Co pins, the situation arose whereby the original Au coating on the pins was not fully dissolved into the Au-Sn solder. Therefore, the Au-Sn solder wetted and bonded directly to the Au finish rather than to the Ni layer. This situation is shown by the SEM photograph in Fig. 10. The Au-Sn solder joints of this unit exhibited excellent pull strengths. The inset photograph shows, in cross-section, the predominant failure mode, which was separation at the thick film/LTCC interface. The enlarged photograph shows that the Au-Sn solder had wetted to the Au layer. There was no indication of cracking or layer delamination along that interface. In effect, the strength of the bond between the Au-Sn solder and Au finish was *higher* than that of the bond between the thick film bond pad and the LTCC substrate.

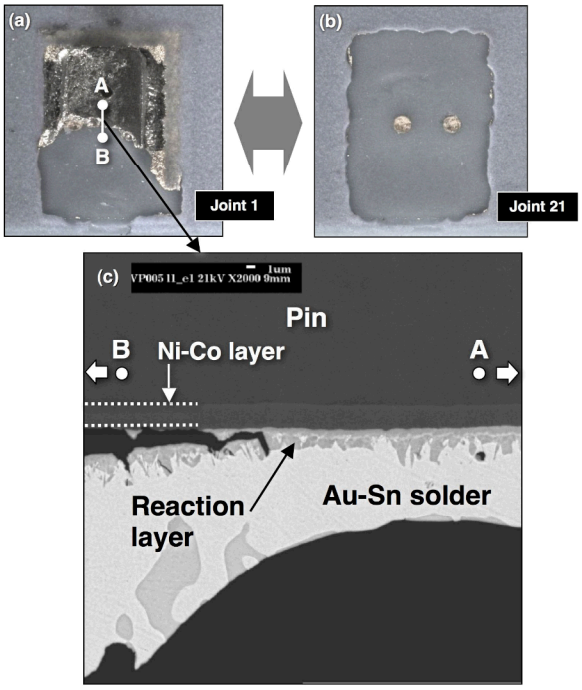

Fig. 9 (a, b) Stereo photographs of pull tested, pin solder joints on a unit made by an alternative vendor, showing the two failure modes: solder/pin separation and thick film/LTCC separation. (c) SEM photograph that captures the crack path when it did occur at the solder/pin interface.

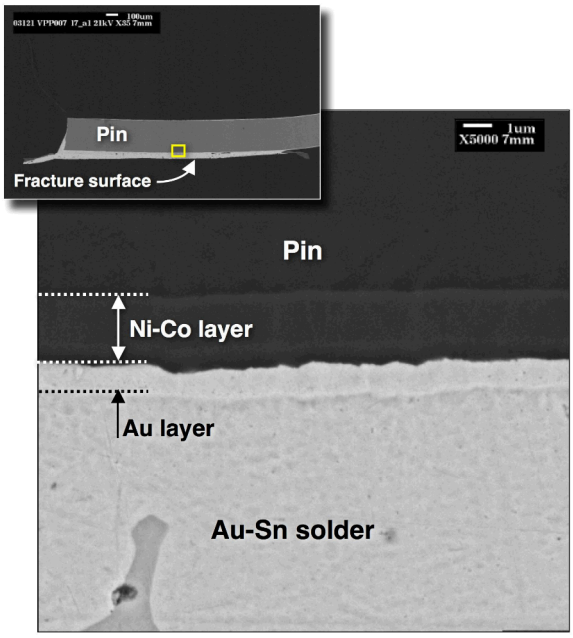

Fig. 10 SEM photograph of the bond at the solder/pin interface in which the Au-Sn solder had not fully dissolved away the Au finish. The inset SEM photograph confirms the failure mode as thick film/LTCC interface separation.

In summary, the images in Figs. 9 and 10, together with the associated pull strength and failure mode analyses, confirmed the following two points: (1) The presence of the reaction layer that formed between the Au-Sn solder and Ni finish was not, intrinsically, a weak structure of the interconnection. (2) The presence of the Au-Sn solder wetting and bonding to the Au finish of the pin, rather than to the underlying Ni layer, did not predispose the solder joint to a low pull strength. These points suggested that the reaction layer that formed between Ni layer of the Cu-Sn-P pins and Au-Sn solder differed from that which formed between the solder and the Ni-Co layer of the Fe-Ni-Co pins.

The test of this hypothesis was performed by the following experiment. Three LTCC substrate units of the same lot number were assembled with three variants of the Cu-Sn-P lead coatings:

1. Original Au layer was stripped; the **original Ni** layer re-activated; and a **new 1.5 µm Au** was electroplated over the original Ni coating. This condition eliminated a potential contamination effect caused by the original Au plating process or layer material.
2. Original Au layer and part of the original Ni layer were stripped; **new 1.8 – 2.5 µm Ni** layer was replated on the pins followed by a **new 1.5 µm Au** finish. This condition eliminated potential effects by both the original Ni and Au coatings. The original Ni layer could not be entirely removed because the stripper chemistry would attack the Cu-Sn-P pin material.
3. Original Au layer was dissolved; the **original Ni** layer was reactivated; and a **new 3.8 µm Au** finish was put on the lead. The objective of this variant was, not only to remove any contamination role of the original Au coating but also, to prevent the Au-Sn solder from reaching the suspect Ni layer and reacting with it by using a thicker Au coating.

The leads were pull tested and failure mode analysis performed on the joints. The strength results of the pull tests (N=26 or 27 data per condition were:

A. **Original Ni; new 1.5 µm Au:** 1.5±0.2 lb.
B. **New 1.8-2.5 µm Ni; new 1.5 µm Au:** 1.9±0.4 lb.
C. **Original Ni; new 3.8 µm Au:** 3.5±0.5 lb.

The case (A) joints exhibited an improvement over the < 1 lb pull strengths on the original units simply by replacing the Au layer. The failure mode was dominated by the solder/pin interface separation as shown in the stereo photograph inset of Fig. 11. The SEM photograph below the inset shows the presence of the reaction layer at the Ni/Au-Sn solder interface. The cracks propagated through this reaction layer.

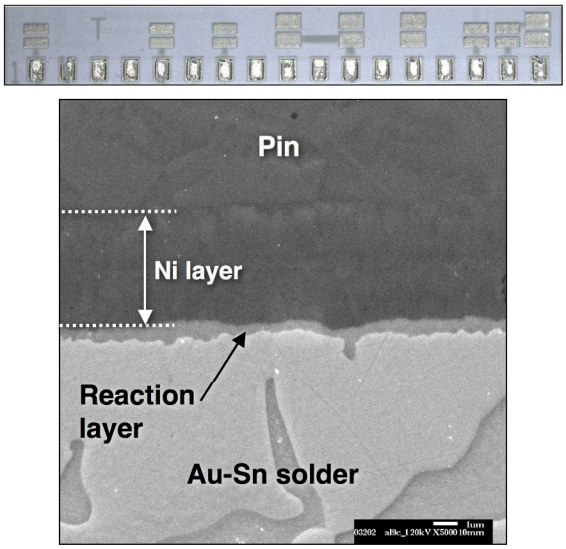

Fig. 11 Inset stereo photograph showing the solder/pin fracture mode that predominated the case (A) pin pull tests. The SEM photograph shows the reaction layer that had formed between the Ni layer and the Au-Sn solder.

Only a modest increase of strength was observed when the entire Au layer and a portion of the original Ni layer were replaced per case (B). The failure modes were very similar to that of case (A) shown in Fig. 11. There was a predominance of the solder/pin interface separation, although the thick film/LTCC failure mode appeared more frequently. There was formation of a reaction layer at the Ni/Au-Sn interface similar to that in Fig. 11.

A significant strength improvement was observed when the original Ni layer was retained, but the Au layer was replaced with a thicker Au coating. The inset stereo photograph in Fig. 12 shows that the predominant failure mode was separation at the thick film/LTCC interface. The SEM photograph of the joint cross section shows the absence of a reaction because the Au-Sn could not fully dissolve away the thicker Au layer and, as such, did not reach the Ni layer.

At this juncture, it was concluded that the reaction layer that formed on the Cu-Sn-P pins was responsible for the low pull strength of the pins. Thickening of the Au layer appeared to be an option because it simply prevented the Au-Sn solder from reaching the Ni layer, thereby eliminating the reaction layer, altogether. Unfortunately, this option was not viable because, at the other end of the pin, the straight lead had to be soldered into a rigid-flex circuit board. Being unable to hot solder dip the lead, there was a substantial risk of joint embrittlement if the leads were soldered (Sn-Pb) directly into the rigid-flex holes in the presence of such a thick Au coating.

The above analysis further substantiated that the role of that reaction layer did not rest with its thickness. Rather, the data suggested that the *composition* of the layer and the integrity of the interface between that phase composition and the Ni layer was the source of the low pull strengths. Therefore, the

compositions of the interface structures were measured using EPMA.

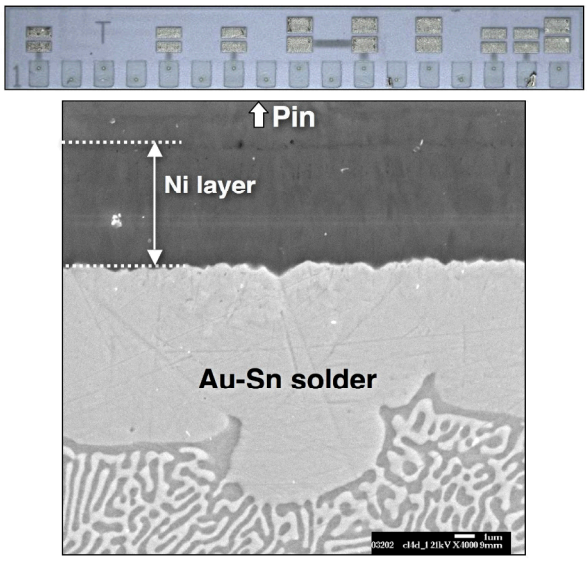

Fig. 12 Inset stereo photograph showing the thick film/LTCC fracture mode that predominated the case (C) pull tests. The SEM photograph shows the absence of the Ni/Au-Sn reaction layer.

Shown in Fig. 13a is the EPMA trace taken across the electroplated layers that were deposited on the Fe-Ni-Co lead. This coating was not in the as-received condition; rather, it had been exposed to the furnace profile used to make the Au-Sn solder joints. A small degree of Fe diffusion had taken place through the Ni-Co layer. Also, there was a small zone of interdiffusion between the Au and the Ni and Co components of the electroplated coating (10 µm location on the x-axis).

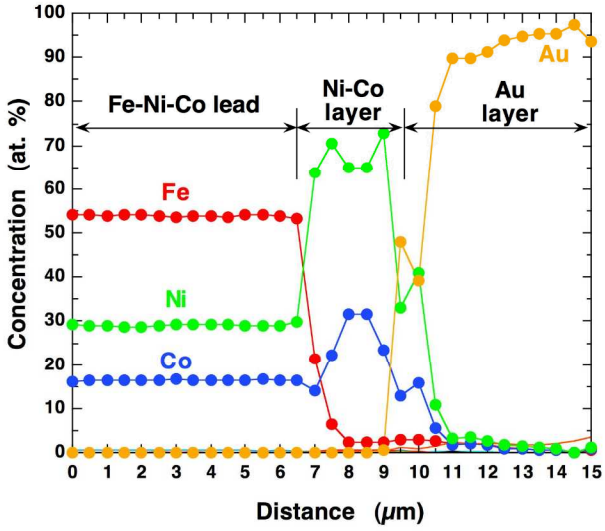

(a)

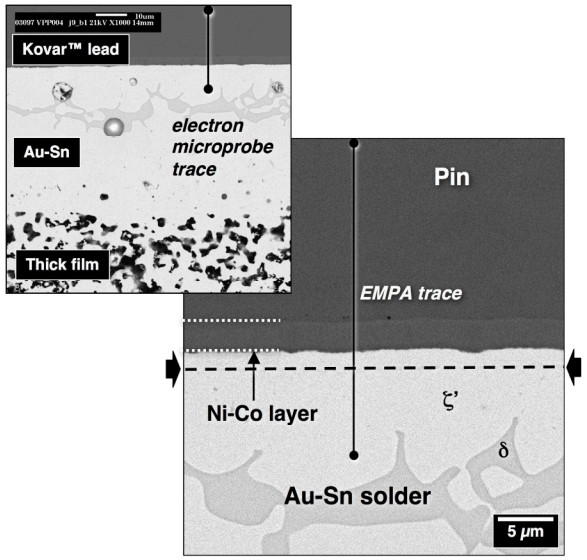

(b)

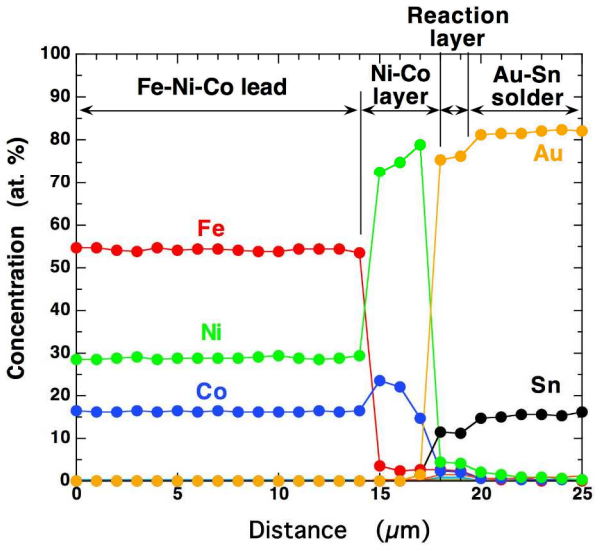

(c)

Fig. 13 (a) EPMA trace through the electroplated layers of the Fe-Ni-Co pin without the Au-Sn solder. (b) SEM photographs showing the location of the EPMA trace through the pin/solder interface. The black block arrows and dashed line indicate the location of the reaction layer. (c) The EPMA trace from the pin into the Au-Sn solder of the actual joint.

The EPMA was also performed across the interface between the pin and the Au-Sn solder of the actual joint. The SEM photographs in Fig. 13b show the location of the trace and the microstructure of the interface. The EPMA trace is shown in Fig. 13c. (Note, there is a different x-axis scale when compared to Fig. 13a.) The Au-Sn solder had fully dissolved the pure Au coating and formed a reaction layer with the original interdiffusion layer between Au, Ni, Co, and Fe that was shown in Fig. 13a. There was only a trace of Ni, Co, and Fe remaining there amidst Sn and Au. The reaction layer composition was based upon the ζ‘ (Au_5Sn) phase, but with

traces of Ni, Co, and Fe likely in solid-solution. Beyond the reaction layer is the ζ‘ terminal phase of the Au-Sn solder. The gray phase in Fig. 13b is the second terminal phase of the Au-Sn eutectic composition, δ, or AuSn.

The same EPMA was performed on the Cu-Sn-P pins. The results of that analysis are presented in Fig. 14. Shown in Fig. 14a is the trace across the electroplated layers, only. Like the Fe-Ni-Co pin case, above, these layers were exposed to the Au-Sn solder process temperature profile, but not to the molten Au-Sn solder. The Ni layer is approximately 2 µm wide. There was a measurable degree of interdiffusion by Ni and Cu (from the lead) into the Au layer. In fact, the Cu had diffused through the Ni layer, accumulated in the Au coating as well as diffused to the surface of the Au layer. At the surface, the Cu concentration was approximately 10 at.%.

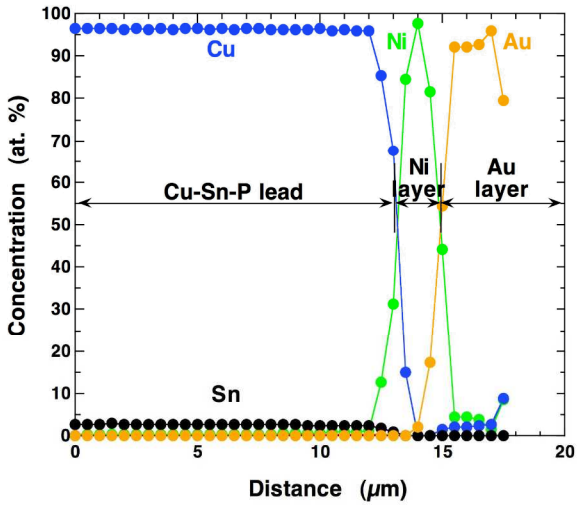

(a)

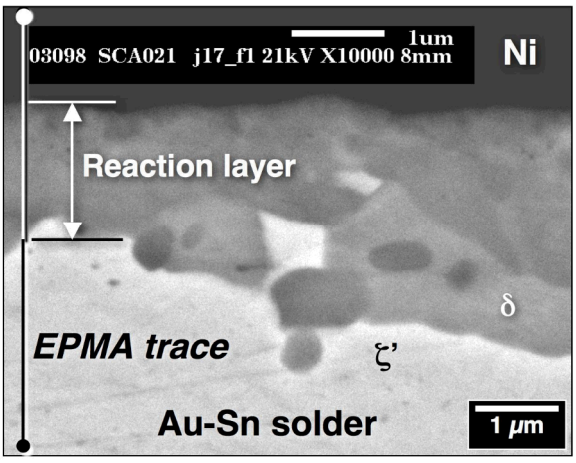

(b)

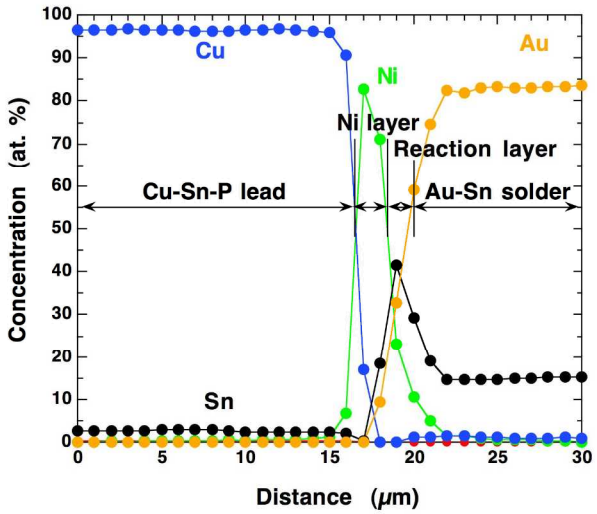

(c)

Fig. 14 (a) EPMA trace through the electroplated layers of the Cu-Sn-P pin without the Au-Sn solder. (b) SEM photograph showing the location of the EPMA trace through the pin/solder interface. (c) The EPMA trace from the pin into the Au-Sn solder of the actual joint.

The location of the EPMA trace that was made through the pin/solder interface on the solder joint side of the pin is shown in Fig. 14b. The two phases, ζ‘ and δ, which comprise the Au-Sn solder, were identified in the image. The other phases of slightly darker gray tones resulted from the reaction between the solder and the Ni coating above it.

The EPMA trace is shown in Fig. 14c, which crossed the interface between the solder and the Cu-Sn-Pb pin. A reaction layer is indicated by the peak in the Sn concentration. The layer composition is $(Au, Ni)_xSn_y$. This compositional arrangement was based upon the assumption that Au and Ni would substitute for one-another due to their extensive mutual solubility as a binary alloy [7]. However, there is no phase of 40 at.% Sn that would have its basis in the binary Au-Sn system. Therefore, it can only be concluded that the reaction layer is a mixture of ζ‘ and δ phases having compositions that included Ni, that is, $(Au, Ni)_5Sn$ and (Au, Ni)Sn, respectively. The mixture of these phases was responsible for the multiple gray tones observed in Fig. 14b. The reaction layer composition is in contrast to that in Fig. 13b (Fe-Ni-Co lead), which was based upon the binary ζ‘ phase, but with small amounts of Ni, Co, and Fe. There was no significant Cu content in the reaction layer in Fig. 14c. There was a trace of Cu in the solder's ζ‘ phase immediately adjacent to the reaction layer.

A closer comparison was made between Figs. 14a and 14c, taking into account the different x-axes scales. In both cases, it was confirmed that there was very little dissolution of the Ni layer. The same observation was made for the case with the Fe-Ni-Co pins (Figs. 13a and 13c).

A correlation can be drawn between the low pull strengths of the Cu-Sn-P pin solder joints and weakening of the joints by formation of the $(Au, Ni)_xSn_y$, reaction layer. The EPMA trace in Fig. 14c indicated that a substantial concentration of Sn (40 at.%) was present in the reaction layer. The Sn did not come from the Cu-Sn-P pin as no depletion region was recorded in the latter's composition profile. Thus, the Sn was drawn to the interface from the Au-Sn solder bulk. In the case of the Fe-Ni-Co pins, there was no apparent driving force for Sn to accumulate into a similar reaction layer at the interface.

The driving force that determined the extent to which Sn was drawn to the interface, depended upon the composition of electroplated layers to which the molten Au-Sn solder wetted. These compositions were reflected by the EPMA traces in Figs. 13a and 14a for the Fe-Ni-Co and Cu-Sn-P pins, respectively. In both cases, there is Ni present in the Au layer, in fact, more so for the Fe-Ni-Co lead. Therefore, the presence of Ni in the layer did not appear to be the primary source of the driving force. It should be mentioned that there is a significant presence of Co in Fig. 13a. In the absence of supporting data, it was assumed that the Co did not "poison" a contributing driving force by Ni towards Sn accumulation at the interface.

The remaining difference between the Au layer compositions in Figs. 13a and 14a is the presence of Cu in the Au layer of the Cu-Sn-P pin. Therefore, it was concluded that Cu, or possibly a synergistic effect between Cu and Ni, provided the added driving force to cause Sn to diffuse from the solder to the interface. Thus, the root-cause of the low pull strengths was the presence of Cu in the Au layer, which had diffused from the Cu-Sn-P pin material. The consequence was formation of the high-Sn, $(Au, Ni)_xSn_y$ reaction layer product (possible mixture of ζ' and δ phases tainted with Ni) at the pin/solder interface, which had poor adhesion to the Ni layer.

This conclusion corroborates the earlier results. Replacement of the Au layer improved the pull strength somewhat. The introduction of the thicker Au layer, not only replaced the original contaminated Au layer, but also prevented a reaction layer from potentially forming at the Ni layer (ref. Fig. 12). Also, an additional series of experiments was performed in which the two different pin materials sets were given to the different suppliers to make the Au-Sn joints. When the original supplier of Cu-Sn-Pb pin assemblies made a test unit with Fe-Ni-Co pins (and associated electroplating layers), excellent pull strengths were realized (mean, 2.4 lb; max., 2.6 lb; min., 2.3 lb). The predominant failure mode was thick film/LTCC separation and the EPMA showed the same compositional profile through the pin/solder interface as that shown in Fig. 13c. Conversely, when the second supplier was asked to solder a unit with the Cu-Sn-P pins, the pins exhibited very low pull strength (mean, 0.87 lb; max., 1.2 lb; min., 0.70). The predominant failure mode was separation at the pin /solder interface and the EPMA showed the same elevated Sn, $(Au, Ni)_xSn_y$ reaction layer and overall composition profile as previously observed with the Cu-Sn-P pin solder joints (Fig. 14c).

Solution

A methodology was sought in order to mitigate the low pull strength behavior. It was not possible to use the Fe-Ni-Co pins; therefore, the strategy required an adaptation of the Cu-Sn-P pins. Per the root-cause analysis, it was necessary to eliminate Cu (or the combination of Cu and Ni) from the electroplated Au layer prior to the soldering process. Therefore, the Cu-Sn-P pin lead frames were stripped of the as-received Au plating layer down to the Ni finish. The latter was re-activated and an additional Ni coating (sulfamate bath) was deposited over the previous Ni layer for a *total* thickness of 3.8 – 6.4 µm. The purpose of the new Ni layer was to provide an additional barrier between the original Ni layer, now contaminated with a Cu diffusion pathway, and the newly deposited Au layer. A new Au layer was deposited to a minimum thickness of 1.6 µm, which would be devoid of Cu (as well as Ni) contamination.

This process proved to be successful. The Au-Sn solder joints assembled with the reconditioned pins exhibited excellent pull strengths; a failure mode that was predominantly at the thick film/LTCC interface; and an absence of the $(Au, Ni)_xSn_y$ reaction layer.

Conclusions

1. A study was conducted, the objective of which, was to identify the root-cause of low pull strengths that were experienced by phosphor bronze (Cu-Sn-P) edge pins on a low-temperature co-fired (LTCC) ceramic substrate. The pins were attached to post-process, fired-on Au thick film bond pads atop the LTCC substrate, using the 80Au-20Sn (wt.%).
2. Failure analysis, using metallographic cross sections, scanning electron microscopy (SEM), and electron-probe microanalysis (EPMA) identified the root-cause of the low pull strengths, which began with the formation of a high-Sn, $(Au, Ni)_xSn_y$ reaction layer at the pin/solder interface. Specifically, the low pull strengths were caused by a weak bond between that reaction layer and the Ni coating.
3. The underlying mechanism was the diffusion of Cu into the Au layer from the Cu-Sn-P pin material. The Cu, either alone or in synergism with a concurrent, low-level Ni contaminant, provided the driving force for excessive Sn to diffuse to the pin/solder interface, resulting in formation of the $(Au, Ni)_xSn_y$ reaction layer.
4. Based upon the failure mode analysis, the following successful mitigation process was established in order to utilize the Cu-Sn-P pins: (a) the original Au coating was stripped from the pin surfaces; (b) the exposed Ni coating was reactivated and then plated over with a new Ni layer (1.5 µm thick); and (c) a new Au layer (1.5 µm) was coated on the pins. The Au-Sn solder joints using these reconditioned pins exhibited excellent pull strength.

Acknowledgments

The authors wish to thank P. Hlava for the electron probe microanalysis work and D. Susan for his careful review of the manuscript.

References

[1] Principles of Soldering and Brazing, by G. Humpston and D. Jacobson (Materials Park, OH; 1993).

[2] Wright, C., "The Effect of Solid-State Reactions Upon Solder Lap Shear Strength," *Proc. 27th Electronic Components Conference*, Arlington, VA, May 1977 pp. 199 – 205.

[3] Yost, F. "Ultimate Strength and Morphological Structure of Eutectic Bonds," *J. Elect. Mater.* Vol. 3 (1974) pp. 353 – 369.

[4] Binary Alloy Phase Diagrams, ed. by T. Massalski, ASM International (Materials Park, OH; 1986) p. 316.

[5] Olsen, D. and Berg, H., "Properties of Die Bond Alloys Relating to Thermal Fatigue," *IEEE Trans.-CHMT*, Vol. CHMT-2, No. 2 (1979) pp. 257 – 263.

[6] Novakivic, R, Ricci, E., Gnecco, F., Giuranno, D., and Borzone, G., "Surface and Transport Properties of Au-Sn Liquid Alloys," *Surf. Sci.* Vol. 599 (2005) pp. 230 – 247.

[7] Massalski, op. cit. p. 289.